Geospatial Health 2022; volume 17:1087

Spatiotemporal patterns of mortality associated with chronic non-communicable diseases and child malnutrition at the municipal level in Mexico

José Mauricio Galeana-Pizaña,[1] Leslie Verdeja-Vendrell,[1] Lizbeth Ixchel Díaz-Trejo,[2] Carlos Anzaldo,[1] Daniela Figueroa,[3] Aldo Daniel Jiménez-Ortega[1]

[1]Research Centre for Geospatial Information Sciences; [2]National Centre for Disease Control and Prevention Programs; and [3]Institute of Geography, National Autonomous University of Mexico, Mexico City, Mexico

Abstract

Malnutrition is one of the main risk factors related to chronic non-communicable diseases and child undernourishment on a planetary scale. Mexico is one of the countries with the highest levels of malnutrition, but there is also an accelerated increase in overweight or obesity. This study explored the spatiotemporal behaviour of mortality associated with chronic non-communicable diseases such as type II diabetes mellitus, hypertension, ischemic heart disease and cerebrovascular disease. The analysis was carried out at the municipality level for the 2000-2020 period targeting two age groups: ≥60-year olds and 20-59-year olds. In addition, 0-4-year olds were investigated with respect to undernourishment. National databases were gathered and standardized for each disease and SaTScan spatiotemporal cluster analyses were performed. We found that mortality associated with most of the diseases evaluated has increased since 2016 except for mortality caused by child undernourishment, which showed a downward trend during the study period. To focus on active conglomerates of diseases is important as they currently represent a threat to public health. Our results contribute to the potential spatial prioritization of the allocation of resources and campaigns for prevention and treatment of chronic non-communicable diseases and child undernourishment. Generally, geographical studies are fundamental for the discovery of disease aetiology and they provide valuable and timely information to multiple stakeholders.

Correspondence: José Mauricio Galeana-Pizaña, Research Centre for Geospatial Information Sciences (CENTROGEO), Contoy 137, Col. Lomas de Padierna, Apdo Postal 14240, Mexico City, Mexico.
E-mail: mgaleana@centrogeo.edu.mx

Key words: Chronic non-communicable diseases; child undernourishment; mortality; space-time clusters; Mexico.

Acknowledgements: the project was supported by CONACYT through FORDECYT-PRONACES with number 10422 entitled '*Dinámica espacio-temporal de la malnutrición desde la perspectiva del sistema agroalimentario 2000-2020'*.

See online Appendix for additional Tables.

Received for publication: 5 March 2022.
Revision received: 19 April 2022.
Accepted for publication: 19 April 2022.

Geospatial Health 2022; 17:1087
doi:10.4081/gh.2022.1087

Introduction

According to World Health Organization (WHO) statistics, 7 out of 10 deaths in 2019 were caused by chronic non-communicable diseases (CNCDs) (WHO, 2021). Among these, ischemic heart disease stands out, followed by cancer, respiratory diseases and diabetes (WHO, 2021). Type II diabetes, arterial hypertension and ischemic heart disease are the main causes of death in Latin America and the Caribbean (Di Cesare, 2011). In the context of the current coronavirus disease 2019 (COVID-19) pandemic, there is an increased risk for middle-aged people and those older than 60 years with chronic diseases, such as diabetes, cardiovascular diseases and hypertension, as this infection is often associated with respiratory failure and significant complications that can lead to death in these age groups (Liu *et al*., 2020). The CNCDs are a challenge for national health systems derived from increases in already high incidence rates, which result in: i) high levels of general mortality; and ii) increase of physical impairment based on the high cost of hospitalization, medical treatment and rehabilitation (Serra Valdés *et al*., 2018). Furthermore, attention to the presence and increase in CNCDs is a key element to mitigate complications and mortality of COVID-19 (Liu *et al*., 2020).

Malnutrition, another CNCD, is one of the greatest public health challenges globally (Gomes, 2019). It is associated with main risk factors (Nugent *et al*., 2020) with repercussions on the health and well-being as well as on physical and cognitive development that often remain throughout affected individuals' life with resonance from one generation to the next (FAO, 2020). Mexico is one of the countries with a high presence of malnutrition and paradoxically also with overweight or obesity. Although these afflictions generally occur in different age groups, they are increasing at an accelerated rate year after year (Urquía-Fernández, 2014). Currently, malnutrition and overweight represent an important 'syndemic' that threatens the country since they impact the number of deaths and the number of years of healthy life lost affecting quality of life and labour productivity (Fernández *et al*., 2017). According to the 2018 *National Survey of Health and Nutrition*, 75.2% of adults over 20 years of age at the national level are overweight or obese, which is an increase of 3.9% compared to the data reported by a corresponding survey carried out in 2012. This dynamic in Mexican young and grown-up people has a direct implication regarding type II diabetes mellitus since 90% of the cases are due to overweight and obesity. Also, this disease is one of the primary causes of death in Mexico, only below that due to heart disease.

In 2018, the following figures were obtained regarding chronic undernourishment in children 0-4 years old: 14.9% had chronic malnutrition, 4.4% were underweight and 1.5% diagnosed as emaciated (Barquera *et al*., 2020). The combination of these aspects of poor nutrition represents 2.3% of the annual gross domestic product (GDP), equivalent to 28.8 billion USD (Fernández *et al*., 2017). These figures highlight the importance of strengthening the institutional capacities of the health system, as well as increasing the efficiency and sectoral coordination of current public policies.

In the late 1990s, technological advances in computer software, such as geographical information systems (GIS), allowed non-random distributions of diseases to be more easily mapped and spatial relationships to be reported with statistical significance (Thurston *et al*., 2017). With the incorporation of data mining in geographic studies, the development of statistical methods for public health and epidemiology has been promoted (Rodríguez *et al*., 2008). This presents potential benefits for epidemiological and health studies. Data mining also offers new opportunities and challenges to discover valuable patterns of information in datasets, among which the analysis of spatiotemporal information stands out (Shi and Pun-Cheng, 2019). There is a wide range of spatio-temporal approaches used for monitoring areas of high epidemiological risk, detection of disease conglomerates, evaluation of spatial variations in temporal trends, early detection of epidemics and in the identification of determining disease risk factors (Moraga, 2017). One of the most commonly used methods is the spatio-temporal scan statistics, which is an extension of spatial statistics to the detection of clusters of disease (Kulldorff, 2001; Kulldorff *et al*., 2005). In Mexico, the use of these methods has been related to the analysis of the spatio-temporal patterns of diseases, *e.g*., tuberculosis (Zaragoza Bastida *et al*., 2012), dengue fever (Hernández-Gaytán *et al*., 2017) and COVID-19 (Mas and Pérez-Vega, 2021; Benita and Gasca-Sánchez, 2021). However, to our knowledge, they have not been used to track CNCD. In this regard, the present study aims to explore the space-time mortality in various age groups and its association with CNCD, such as type II diabetes mellitus, arterial hypertension, ischemic heart disease and cerebrovascular disease as well as child undernourishment.

Materials and methods

Data sources

Information on population and housing was obtained from censuses of the '*Instituto Nacional de Estadística y Geografía*' (INEGI), *i.e*. the National Institute of Statistics and Geography in Mexico. We consolidated a time series of 21 years (2000 to 2020) at the municipal level. The study was carried out using time series with data reported on death certificates provided by the '*Dirección General de Información en Salud'* (DGIS) - Ministry of Health in Mexico (DGIS, 2020). We based our study on the cause of death on the certificates coded according to the tenth version of the International Classification of Diseases (ICD-10) as follows: i) child undernourishment: E40X, E41X, E42X, E43X, E44, E45X, E46X; ii) type II diabetes mellitus: E11, E110, E111, E112, E113, E114, E115, E116, E117, E118, E119; iii) arterial hypertension: I10; iv) ischemic heart disease: I20, I21-122, I23-I25; and v) cerebrovascular disease: I60-I67 and I69.

Access to the DGIS data was achieved through the dynamic cubes platform, an electronic repository of the integrated national database. This platform contains data from different periods related to the information reported from death certificates. For the analyses, only the records from 0 to 4 years were selected for deaths associated with child undernourishment, while two age ranges were selected for the other CNCDs: one including the 20-59-year olds and another for the ≥60-year olds. The same time intervals for the series of deaths and that regarding population information and housing were used for the age groups selected. The study was thus based on the censuses of 2000, 2010 and 2020 together with inter-census surveys of 2005 and 2015 published by INEGI.

Data standardization

According to the Population and Housing Censuses counts, the municipalities in Mexico increased from 2443 units in 2000 to 2469 units in 2020. To calculate the population of these municipalities prior to their creation, we reviewed the geographical location of the country's localities in census and inter-census years covering the years 2000, 2005 and 2010 with respect to the existing municipal division in 2020. The population data of each locality were subtracted from the municipality's total population to which it belonged, so only a redistribution of the population of the original year was carried out. The disease databases were standardized with reference to the 2020 national statistical framework based on these factors.

Once the population database was standardized, a demographic reconciliation was carried out to harmonize the trends of the components of demographic change with the population by age, listed in the censuses from which the base population of the mid-year population projections was determined. For the demographic reconciliation, the population proportion of each municipality to the state total was estimated for each census and inter-census event between 2000 and 2020. In this sense, for each municipality, the proportion $w_{i,t}$ represented of the respective state population in 2000, 2005, 2010, 2015 and 2020 was obtained. Subsequently, these proportions were linearly interpolated to estimate the share corresponding to each year, and the estimated annual proportions were multiplied by the population data, clustered into five-year age groups for each state to obtain the equivalent estimates at the municipal level.

Being P_t and P_{t+5} the total populations at state level in two consecutive censuses and inter-census events (*e.g*., 2000 and 2005), and $p_{i,t}$ and $p_{i,t+5}$ the corresponding figures at municipality level, as shown in Equation 1.

$$P_t = \sum_{i=1}^{n} p_{i,t} \text{ and } P_{t+5} = \sum_{i=1}^{n} p_{i,t+5} \text{ for } t = 2000, 2005, 2010, 2015. \quad (1)$$

The census and inter-census municipality proportions, $w_{i,t}$ and $w_{i,t+5}$ were calculated as shown in Equation 2.

$$w_{i,t} = p_{i,t}/P_t \quad \text{and} \quad w_{i,t+5} = p_{i,t+5}/P_{t+5} \tag{2}$$

The annual proportions between each five-year period were calculated as shown in Equation 3.

$$w_{i,t+a} = w_{i,t} + \left(a * \frac{w_{i,t+5} - w_{i,t}}{5}\right) \quad \text{for} \quad a = 1, 2, 3, 4. \tag{3}$$

Mid-year population figures, from t = 2000, 2001, 2002, …, 2020, at the municipal level were estimated as shown in Equation 4.

$$h_{j,t} = w_{i,t} * H_{j,t} \quad m_{j,t} = w_{i,t} * M_{j,t} \quad \text{for:} \quad t = 2000, 2001, 2002, \ldots 2020. \tag{4}$$

where H is the number of men; and M the number of women in the middle of year t for the five-year age group j at the federal entity level, from the demographic reconciliation and population projections (CONAPO, 2018).

Statistical analysis

The retrospective space-time scanning statistical method (Kulldorff *et al*., 1998) was used to include the time dimension in the analysis for each CNCD and to identify where and when (and for how long) clusters occurred. A discrete Poisson model was used to analyse spatio-temporal clusters of type II diabetes mellitus, hypertension, ischemic heart disease, cerebrovascular disease, and childhood malnutrition in SaTScan v. 10.0 (Kulldorff and Information Management Services Inc., 2018).

The scan window for space-time statistics is cylindrical, with a circular geographic base and height corresponding to time (Kulldorff *et al*., 1998). The base is centred around one of the possible centroids placed on the spatial units, with a radius varying from zero to a specified maximum value. The height reflects any possible time interval, including the entire study period and the interval less than or equal to half the study period. In this study, one year was selected as the time interval. The maximum spatial cluster size was set at 5% of the population at risk and the maximum temporal cluster size was set at 25% of the total period length (five years) to avoid enormous clusters. In addition, the minimum number of cases in a high-rate group was set at 30.

A likelihood ratio test was used to identify spatiotemporal clusters of each CNCD under study. The expected and observed cases were calculated for each cylinder considering null hypothesis H_o: 'There is no difference in the risk of each disease between the interior and exterior of the cylinder', and as an alternative hypothesis H_A: 'There is a greater risk of diseases within the cylinder.' The number of expected cases μ was calculated using Equation 5.

$$\mu = p * \frac{C}{P} \tag{5}$$

where p stands for the population of the age range x within the cylinder; C for the total number of deaths within the range x; and P for the total population of the age range x observed in the spatial entities (municipalities) during a particular period (Linton *et al*., 2014). The observed to expected cases ratio represents the risk within the cylinder, and the relative risk (RR) represents the risk within the cylinder compared to the risk outside the cylinder (Linton *et al*., 2014). The RR was estimated with a likelihood ratio test from Equation 6.

$$\frac{L(Z)}{L_0} = \frac{\left(\frac{n_Z}{\mu(Z)}\right)^{n_Z} \left(\frac{N - n_Z}{N - \mu(Z)}\right)^{N - n_Z}}{\left(\frac{N}{\mu(T)}\right)^{N}} \tag{6}$$

where $L(Z)$ is the likelihood function for a cylinder Z; L_0 the likelihood function for H_0; n_z the number of cases within the cylinder; $\mu(Z)$ the number of expected cases in cylinder Z; N the number of cases observed for the entire study area during the period; and $\mu(T)$ the total number of cases expected in the entire study area through all periods of study. The cylinder with the highest likelihood ratio represents the most likely cluster (Hohl *et al*., 2020). The statistical significance was set at 95% and evaluated using a Monte Carlo simulation consisting of 999 random replicates of the dataset (Kulldorff and Nagarwalla, 1995). The spatial representation of the results was carried out through GIS software.

Results

From the causes of death analysed up to December 31, 2020, ischemic heart disease represented the largest number, with an accumulation of registered cases in the period amounting to 1,493,045, 82.9% of which were observed in ≥60-year olds and the remaining 17.1% in adults between 20 and 59 years old. The second cause of death was type II diabetes mellitus with 1,063,645

Table 1. Age group and cause of death for the municipalities with the highest number of accumulated cases in the study period.

Cause of death	Municipality, State (deaths in age group 20-59 years)	Municipality, State (deaths in age group ≥60 years)	Municipality, state (deaths in children ≤4 years old)
Ischemic heart disease	Tijuana, Baja California (n=4510)	Gustavo A. Madero, Ciudad de México (n=22,402)	
Type II diabetes mellitus	Iztapalapa, Ciudad de México (n=7154)	Iztapalapa, Ciudad de México (n=18,740)	
Cerebrovascular diseases	Iztapalapa, Ciudad de México (n=962)	Monterrey, Nuevo León (n=4727)	
Hypertension	Reynosa, Tamaulipas (n=230)	Nopalucan, Puebla (n=1637)	
Child undernourishment			Toluca, Estado de México (266)

cases (74.1% and 25.9%, respectively), followed by 300,430 deaths by cerebrovascular disease (84.5% and 15.5%, respectively) and 114,545 by hypertension (89.3% and 10.7%). Regarding child undernourishment, the accumulated cases were 13,346. Table 1 shows the municipalities with the highest number of accumulated cases according to the cause of death and age group.

Ischemic heart disease

Population ≥60 years old

Sixteen statistically significant clusters were identified for this population in the study period (Figure 1). The clusters were configured by colours based on the identified time frame. According to the likelihood ratio, the conglomerate with the highest value (cluster 1) was located in Comonfort, Guanajuato and 42 other municipalities, with 24,014 cases and RR of 1.710 for the 2016-2020 interval. The 2016-2020 period showed ten conglomerates followed by 2020 with five and 2019-2020 with one. As seen in Table S1 (Appendix), the highest estimated RR was observed in conglomerate 5, with 2.062 located in Huehuetlán El Grande, Puebla and 193 other municipalities that covered a large percentage of the states of Puebla and Tlaxcala.

Population aged 20 to 59 years

Fourteen significant clusters were identified for the 20-59 years old population (Figure 2). The conglomerate with the highest likelihood value (cluster 1) was located in Camargo, Tamaulipas and 46 other municipalities, with 6434 cases and RR of 1.972 for 2016-2020. The highest estimated RR was observed in conglomerate 8 with 2.26 related to Otzolotepec, Estado de México and 29 other municipalities (Table S2).

Type II mellitus diabetes

Population ≥60 years old

Twenty-one statistically significant clusters were identified (Figure 3). The conglomerate with the highest likelihood value (cluster 1) was located in Santa Catarina Ayometla, Tlaxcala and 170 other municipalities, with 23,427 cases and RR of 1.907 for 2016-2020. Likewise, 17 conglomerates were concentrated in the last five years of the analysis period: 11 conglomerates for the 2016-2020 period and six in 2020. The other four conglomerates were registered between 2012 and 2018. The highest estimated RR was observed in conglomerate 15 with 3.299 related to the municipality of Acuña, Coahuila (Table S3).

Population aged 20 to 59 years

Thirteen statistically significant clusters were identified in the study period (Figure 4). The conglomerate with the highest likelihood value (cluster 1) was located in Tenango del Aire, Estado de México, with 28 other municipalities, with 7723 cases and RR of 2.276 for the 2016-2020 interval. The last five years of the analysis period showed ten conglomerates for 2016-2020 and three conglomerates in 2020. The highest estimated RR was observed in conglomerate 8 with 2.93 related to Juárez, Chihuahua and two other municipalities (Table S4).

Cerebrovascular disease

Population ≥60 years old

Twelve statistically significant clusters were identified in the study period (Figure 5). The conglomerate with the highest likelihood value (cluster 1) was located in San Martín Itunyoso, Oaxaca and 621 other municipalities, with 1951 cases and RR of 2.724 for 2020. This cluster showed the highest RR estimated (Table S5). Likewise, eleven clusters were identified for 2020 and another in the 2001-2005 period.

Population aged 20 to 59 years

Fourteen statistically significant clusters were identified in the study period (Figure 6). The conglomerate with the highest likelihood value (cluster 1) was located in Lamadrid, Coahuila and 56 other municipalities, with 386 cases and RR of 3.246 for 2020. Thirteen clusters corresponded to 2020 and one to the 2001-2004 interval. The highest estimated RR was observed in conglomerate 10 with 13.782 located in Chicontepec, Veracruz (Table S6).

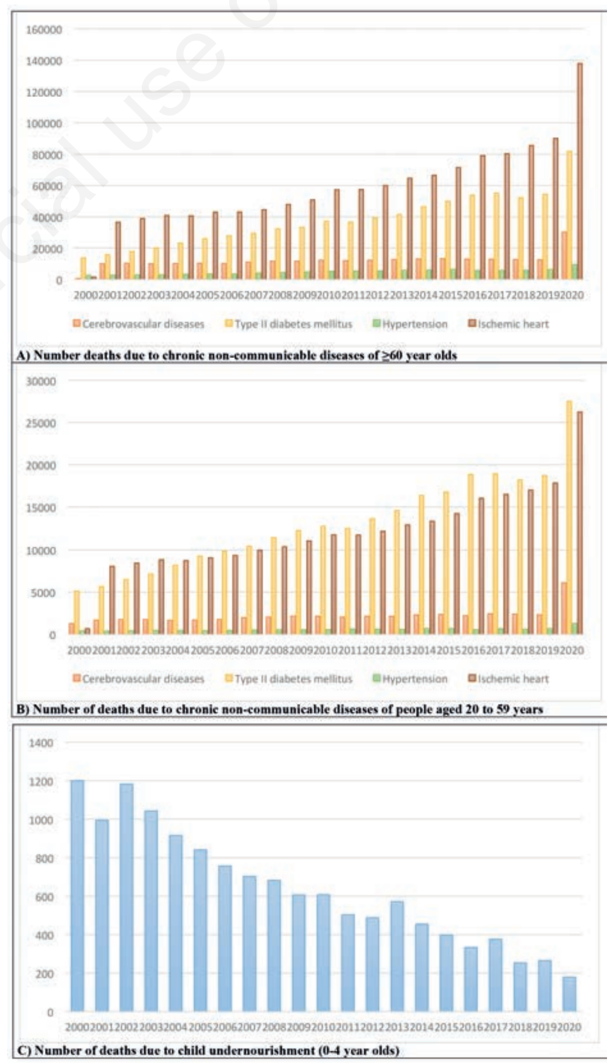

Figure 1. Number of deaths due to chronic non-communicable diseases at the national level.

Figure 2. Space-time clusters of mortality from ischemic heart disease in the ≥60 years old population.

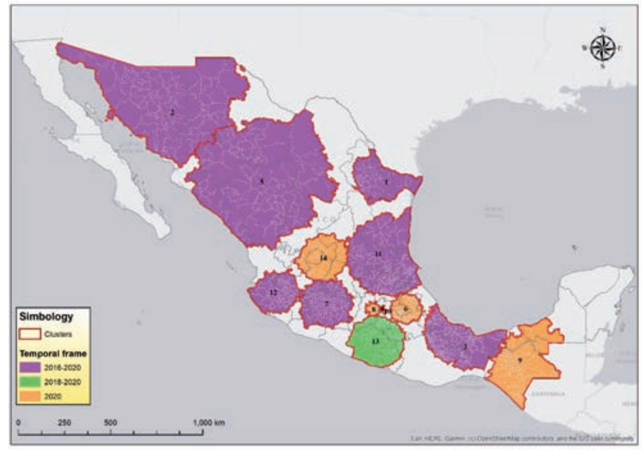

Figure 3. Space-time clusters of mortality from ischemic heart disease in the 20-59 years old population.

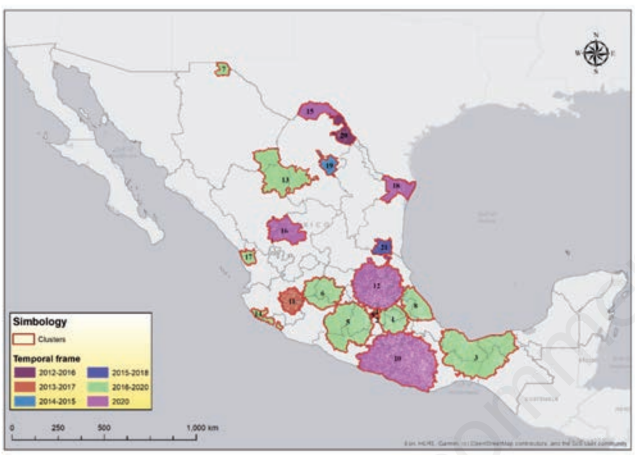

Figure 4. Space-time clusters of mortality of type II diabetes mellitus in the ≥60 years old population.

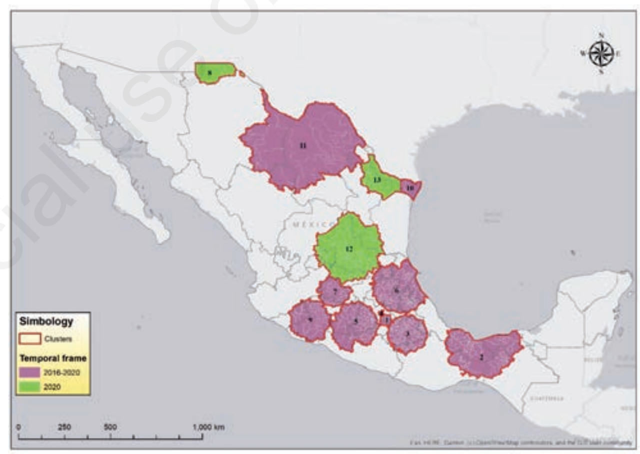

Figure 5. Space-time clusters of mortality of type II diabetes mellitus in the 20-59 years old population.

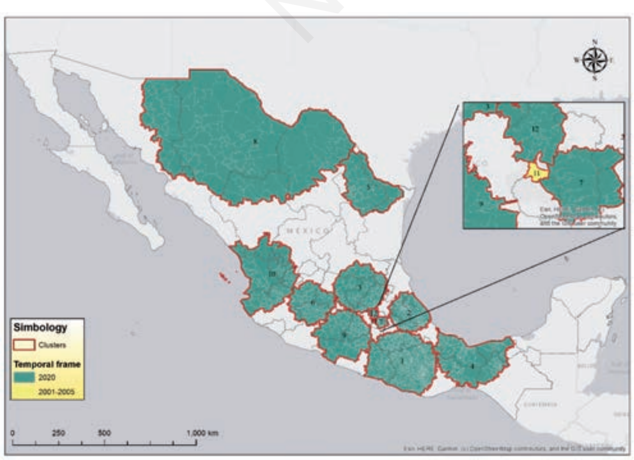

Figure 6. Space-time clusters of mortality of cerebrovascular diseases in the ≥60 years old population.

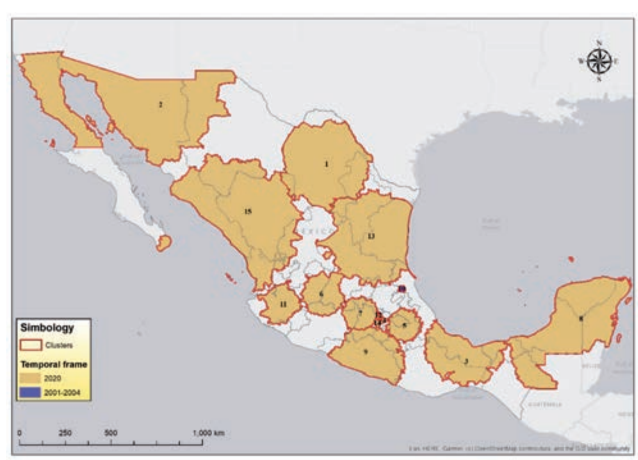

Figure 7. Space-time clusters of mortality of cerebrovascular diseases in the 20-59 years old population.

Hypertension

Population ≥60 years old

Sixteen statistically significant clusters were identified in the study period (Figure 7). The conglomerate with the highest likelihood value (cluster 1) was Sitio de Xitlapehua, Oaxaca and 520 other municipalities, with 2638 cases and RR of 2.682 for the 2016-2020 interval. This disease showed the highest temporal diversity in the clusters identified, with nine time-frames. In addition, a clusters concentration was seen in the last five years, with eight conglomerates. The highest estimated RR was observed in conglomerate 15, with 3.573 related to the municipality of Hualulco de Mercado, Jalisco and three other municipalities (Table S7).

Population aged 20 to 59 years

Nine statistically significant clusters were identified in the study period (Figures 8 and 9). The conglomerate with the highest likelihood value (cluster 1) was located in Balancán, Tabasco and 86 other municipalities, with 296 cases and RR of 3.173 for 2017-2020. A cluster concentration was seen in the last five years, with six conglomerates. The highest estimated RR was observed in conglomerate 3, with 9.388, associated with San Buenaventura, Coahuila and 32 other municipalities (Table S8).

Child undernourishment

Ten statistically significant clusters were identified in the study period (Figure 10). The conglomerate with the highest value (cluster 1) was located in Amanalco, Estado de México and 78 other municipalities, with 677 cases and RR value of 5.075. A clusters concentration was seen in the 2001-2005 period, with eight conglomerates. The highest estimated RR was observed in conglomerate 4 with 14.672 located in Guachochi, Chihuahua and 12 other municipalities (Table S9).

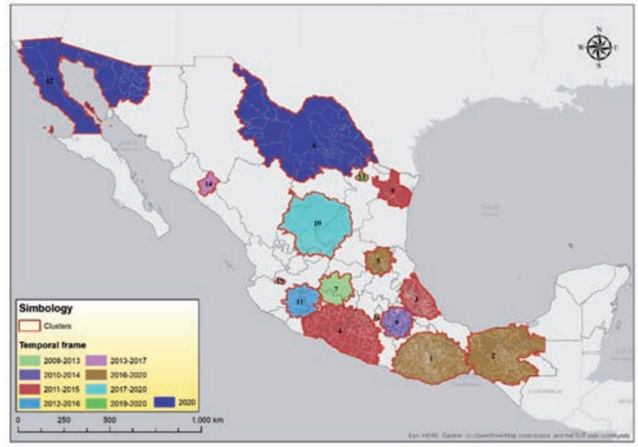

Figure 8. Space-time clusters of mortality of hypertension in the ≥60 years old population.

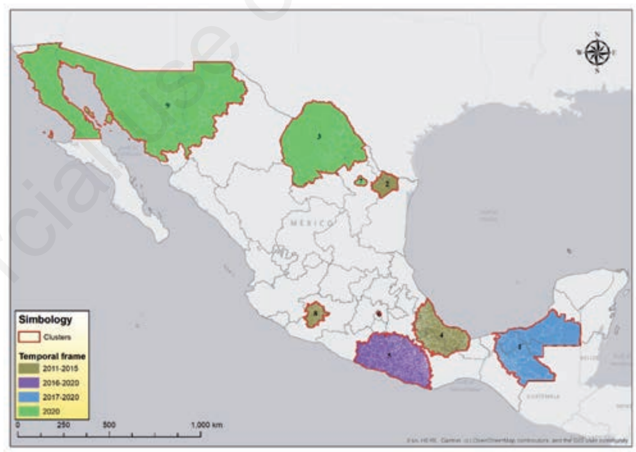

Figure 9. Space-time clusters of mortality of hypertension in the 20-59 years old population.

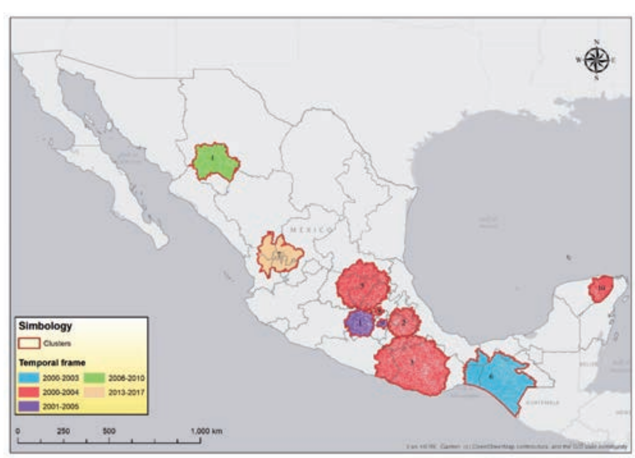

Figure 10. Space-time clusters of mortality due to undernourishment in 0-4 years old children.

Discussion

According to the Organization for Economic Cooperation and Development (OECD), Mexico is one of the three countries with the highest prevalence of diabetes, overweight and obesity (OECD, 2017). Likewise, it is the only OECD country where ischemic heart disease mortality rates have increased from 2000 to 2017, directly related to rising rates of obesity and diabetes (OCDE, 2020).

Our study focused on the municipality level and is expected to contribute to reducing the information gap in the reported for the different municipalities in Mexico, since the researches in the country are predominantly at the national scale (Dávila-Cervantes, 2020; Vázquez *et al*., 2018; Dávila-Cervantes and Pardo-Montaño 2017; Gutiérrez *et al*., 2016; Córdova-Villalobos *et al*., 2008). This contribution could represent the baseline for planning the approach to CNCD and child undernourishment in Mexico, since it would allow the decision-making to be focused on a spatial administrative scale (*e.g*., the municipalities). Our results provide evidence that geographic variation in mortality from the CNCDs could be attributed to demographic structures and possible socioenvironmental factors underlying the clustered pattern found. For example, changes in lifestyle, such as a sedentary lifestyle and poor diet, are part of the problem (Lozano *et al*., 2014). In other words, a large proportion of these diseases are multifactorial, the result of the accumulation of damage caused by obesity, which is a risk factor for the development of diabetes and hypertension and, in turn, for ischemic disease. In addition, cardiovascular diseases continue to be the main cause of morbidity and mortality, which impacts health costs.

Another important factor that coexists with poor nutritional status is food insecurity, which affects 55.5% of the Mexican population and is related to the consumption of high in energy, saturated fats and deficient in micronutrients food, resulting from economic restrictions (Shamah *et al*., 2020). This factor can increase the risk of mortality in the country's population. Although Mexico has a great biological and cultural diversity that is reflected in the variety of food and ways of cooking them, characteristics of the regions in which it is produced or harvested, its availability and consumption, in some, depends on socioeconomic conditions, which impacts the health status of the population. For this reason, the Knowledge and Use of Biodiversity National Commission (CONABIO) proposed the *Good eating regional baskets* initiative to collect information on said diversity and recognize and treasure such agrobiodiversity linked to the customs and identity of the different regions of the country (CONABIO, 2021).

Considering the economic aspect, Macías Sánchez and Villareal Paéz (2018) reports through models of probability of disease, treatment and the average disease cost, that the public spending incurred by the government through the institutions that provided health services for 2015 amounted to 17,900 million pesos for diabetes and to 52,600 million pesos for hypertension. In total, they add up to 70,500 million pesos, which represents around 14.4% of the budget allocated to health functions in the Federation's Expenditure Budget for 2015 and 22.3% of the subfunction *Provision of health individual services*, which includes care for chronic diseases. In 2021, the Public Health Policy prioritized the control of type II diabetes mellitus, allocating part of the federal budget to the social program *Prevention and control of overweight, obesity and diabetes*, which amounted to 453.58 million pesos, 39.8 million of which were earmarked for professional services (SHCP, 2021).

One of the highlights of this study is the use of comprehensive data from the national death certificates. Aggregating mortality from type II diabetes mellitus, hypertension, ischemic heart disease, cerebrovascular disease and childhood malnutrition can provide helpful information to health planners, policymakers, and researchers on potential determinants of poor nutrition. Our analysis at the municipality level supports the targeting and prioritization of prevention and treatment initiatives since it disaggregates at the said administrative scale the real mortality rates that are usually higher than those reported with respect to the state and national averages.

Despite the contributions of this study and its potential uses as a baseline for future analyses, there are some limitations and assumptions. First, we used the prospective space-time statistics in its basic form, which generates circular clusters. Circles may be a poor choice in a study area with substantial spatial heterogeneity. Second, some of the identified clusters were found to be very large and of limited value for CNCD mitigation. As a result, they can present a considerable variation of risk within them, so it is advisable to carry out local analyses, which can better help identify communities and regions at risk. Therefore, to carry out a complementary and context-specific analysis, future research should incorporate spatial panel-type models with different sets of covariates. This type of model was not included in this work because the dynamics of the spatiotemporal variation of mortality were captured through conglomerate analysis. The general trend showed that both results were sufficient to fulfil the stated objective.

Using public data on CNCD mortality and child undernourishment in Mexico, provided by the DGIS, a cluster analysis was performed, from which we obtained statistically significant clusters reflecting the space-time dynamics of mortality associated with the diseases evaluated at the municipality level for the study period (2000-2020). We found that most of the statistically significant clusters were predominantly gathered in the 2016-2020 period and that the clusters increased in size over time, meaning that since 2016 there has been an increase at the municipality level in cases of mortality associated with most of the diseases evaluated, except for mortality caused by child undernourishment that actually showed a decreasing trend in their number and size over time.

Conclusions

The municipalities-cities that had the highest number of accumulated death cases for the evaluated diseases during the study period were: Tijuana (Baja California), Iztapalapa and Gustavo. A. Madero (Ciudad de México), Reynosa (Tamaulipas), Monterrey (Nuevo León), Nopalucan (Puebla) and Toluca (Estado de México). Likewise, the municipalities with the highest RR associated with ischemic heart disease were: Huehuetlán el Grande, Puebla (for the ≥60 year olds) and Otzolotepec, Estado de México (for the 20-59 year olds). In relation to type II diabetes mellitus, those with the highest risk were: Acuña, Coahuila (for the ≥60 year olds) and Juárez, Chihuahua (for the 20-59 year olds) and with regard to cerebrovascular diseases: San Martín Itunyoso, Oaxaca (for the ≥60 year olds) and Chicontepec, Veracruz (for the 20-59 year olds). With respect to hypertension: Ahualulco de Mercado, Jalisco (for the ≥60 year olds) and San Buenaventura, Coahuila (for the 20-59 year olds). Finally, the Guachochi, Chihuahua municipality was the one with the highest risk of child undernourishment.

Our results contribute to the potential spatial prioritization of resources and campaigns for the prevention and treatment of CNCD and child undernourishment. Focusing on active conglomerates is important for the country since these currently represent a threat to public health. It is essential to clarify the various factors influencing their spatial distribution associated with malnutrition as well as contextual factors, such as the use of health services, consumption patterns, dietary styles and preferences, income level and education. Future analyses are needed to provide relevance beyond the actual geographical distribution of CNCD and child undernourishment by focusing on associated causes and possible solutions. These aspects will be particularly useful for specialists and decision-makers as they can lead to interventions to be targeted to minimize patient susceptibility and optimize and improve disease management effectively. Generally, geographic studies such as this one are essential for the aetiology of diseases because they provide ways and means to rapidly inform a wide diversity of governmental and non-governmental decision-makers.

References

Barquera S, Hernández-Barrera L, Trejo-Valdivia B, Shamah T, Campos-Nonato I, Rivera-Dommarco J, 2020. Obesidad en México, prevalencia y tendencias en adultos. Ensanut 2018-2019. Salud Públ México 62(6).

Benita F and Gasca-Sanchez F, 2021. The main factors influencing COVID-19 spread and deaths in México: A comparison between phases I and II. Appl Geogr 134:102523.

Comisión Nacional para el Conocimiento y Uso de la Biodiversidad (CONABIO), 2021. Canastas regionales del bien comer. Available from: https://www.biodiversidad.gob.mx/diversidad/alimentos/canastas-regionales Accessed: December 14, 2021.

Consejo Nacional de Población (CONAPO), 2018. Proyecciones de la Población de México y de las Entidades Federativas, 2016-2050 y Conciliación Demográfica de México, 1950-2015. Available from: https://www.gob.mx/conapo/acciones-y-programas/conciliacion-demografica-de-México-1950-2015-y-proyecciones-de-la-poblacion-de-México-y-de-las-entidades-federativas-2016-2050 Accessed: July 27, 2021.

Córdova-Villalobos JÁ, Barriguete-Meléndez JA, Lara-Esqueda A, Barquera S, Rosas-Peralta M, Hernández-Ávila M, León-May ME, Aguilar-Salinas CA, 2008. Las enfermedades crónicas no transmisibles en México: sinopsis epidemiológica y prevención integral. Salud Públ México 50:419-27.

Dávila-Cervantes CA and Pardo-Montaño AM, 2017. Cambios en la esperanza de vida por causas de muertes crónicas en adultos mayores. México 2000-2013. Rev Cienc Salud 15:223-35.

Dávila-Cervantes CA, 2020. Tendencia e impacto de la mortalidad por enfermedades cardiovasculares en México, 1990-2015. Rev Cubana Salud Públ 45:1-18.

Di Cesare M, 2011. El perfil epidemiológico de América Latina y el Caribe: desafíos , límites y acciones. CEPAL, Santiago de Chile [Internet]. Comisión Económica para América Latina y el Caribe (CEPAL). Available from: http://www.eclac.org/publicaciones/xml/9/44309/lcw395.pdf

DG de I en S (DGIS), 2020. Subsistema de Prestación de Servicios. Cubos dinámicos de Servicios Otorgados SIS. México: Secretaría de Salud. Available from: http://www.dgis.salud.gob.mx/contenidos/basesdedatos/da_defunciones_gobmx.html Accessed: August 10, 2020.

FAO, FIDA, OMS, PMA and UNICEF,2020. El estado de la seguridad alimentaria y la nutrición en el mundo 2020. Transformación de los sistemas alimentarios para que promuevan dietas asequibles y saludables. FAO, Rome, Italy.

Fernández A, Martínez R, Carrasco I, Palma A, 2017. Impacto social y económico de la doble carga de la malnutrición: modelo de análisis y estudio piloto en Chile, el Ecuador y México. Available from: https://repositorio.cepal.org/bitstream/handle/11362/42535/1/S1700443_es.pdf

Gasca-Sánchez FM, Santos-Guzmán J, Elizondo-Dueñaz R, Mejía-Velázquez GM, Ruiz-Pacheco C, Reyes-Rodríguez D, Rojas-Martínez A, 2019. Spatial clusters of children with cleft lip and palate and their association with polluted zones in the Monterrey metropolitan Area. Int J Environ Res Public Health 16:2488.

Gomes F, Baumgartner A, Bounoure L, Bally M, Deutz NE, Greenwald JL, Schuetz P, 2019. Association of nutritional support with clinical outcomes among medical inpatients who are malnourished or at nutritional risk: an updated systematic review and meta-analysis. JAMA Netw Open 2:e1915138.

Gutiérrez JP, García-Saisó S, Espinosa-de la Peña R, Balandrán DA, 2016. Desigualdad en indicadores de enfermedades crónicas y su atención en adultos en México: análisis de tres encuestas de salud. Salud Públ México 58:666-75.

Hernández-Gaytán SI, Díaz-Vásquez FJ, Duran-ArenasLG, CervantesML, Rothenberg SJ, 2017. 20 years spatial-temporal analysis of dengue fever and haemorrhagic fever in Mexico. Archiv Medical Res 48:653-62.

Hohl A, Delmelle EM, Desjardins MR, LanY, 2020. Daily surveillance of COVID-19 using the prospective space-time scan statistic in the United States. Spatial Spatiotemp Epidemiol 34:100354.

Kulldorff M, Nagarwalla N, 1995. Spatial disease clusters: detection and inference. Stat Med 14:799-810.

Kulldorff M, AthasWF, Feurer EJ, Miller BA, Key CR, 1998. Evaluating cluster alarms: a space-time scan statistic and brain cancer in Los Alamos, New Mexico. Am J Public Health 88:1377-80.

Kulldorff M, 2001. Prospective time periodic geographical disease surveillance using a scan statistic. J R Stat Soc Ser A (Stat Soc) 164:61-72.

Kulldorff M, Heffernan R, Hartman J, Assunçao R, Mostashari F, 2005. A space-time permutation scan statistic for disease outbreak detection. PLoS Med 2:e59.

Kulldorff and Information Management Services Inc, 2021. SaTScan version 10: software for the spatial, temporal and space-time scan statistics [Internet]. Available from: https://www.satscan.org/

Linton SL, Jennings JM, Latkin CA, Gomez MB, Mehta SH, 2014. Application of space-time scan statistics to describe geographic and temporal clustering of visible drug activity. J Urban Health 91:940-56.

Liu H, Chen S, Liu M, Nie H, Lu H, 2020. Comorbid chronic diseases are strongly correlated with disease severity among COVID-19 patients: a systematic review and meta-analysis. Aging Dis 11:668.

Lozano R, Gómez-Dantés H, Pelcastre B, Ruelas MG, Montañez JC, Campuzano JC, Franco FGJ, 2014. Carga de Enfermedades en México, 1990-2010. 148:148-62.

Macías Sánchez, A., and Villarreal Páez, H. J. 2018. Sostenibilidad del gasto público: Cobertura y financiamiento de enfermedades crónicas en México. Ensayos. Rev Econ 37:99-133.

Mas JF and Pérez-Vega A, 2021. Spatiotemporal patterns of the COVID-19 epidemic in México at the municipality level. PeerJ 9:e12685.

Moraga P, 2017. SpatialEpiApp: A Shiny web application for the analysis of spatial and spatio-temporal disease data. Spatial Spatiotemp Epidemiol 23:47-57.

Nugent R, Levin C, Hale J, Hutchinson B, 2020. Economic effects of the double burden of malnutrition. Lancet 395:156-64.

Organización para la Cooperación y el Desarrollo Económicos (OCDE), 2020. Panorama de la Salud 2019: OCDE indicadores. Conifarma [Internet]. Available from: https://www.oecd.org/health/Panorama-de-la-Salud-2019.pdf

Rodríguez MA, Herrera M, Abalo RG, 2008. Las técnicas de estadística espacial en la investigación salubrista. Caso síndrome de Down. Rev Cubana Salud Públ 34:1-11.

Serra Valdés M, Serra Ruíz M, Viera García M, 2018. Las enfermedades crónicas no transmisibles: magnitud actual y tendencias futuras. Rev Finlay 8:140-8.

Shamah LT, Cuevas NL, Romero MM, Gaona PEB, Gómez ALM, Mendoza AL,(2020). Encuesta Nacional de Salud y Nutrición 2018-19. Resultados Nacionales [Internet]. Instituto Nacional de Salud Pública, 268 pp. Available from: https://ensanut.insp.mx/encuestas/ensanut2018/informes.php

Shi Z and Pun-Cheng LS, 2019. Spatiotemporal data clustering: a survey of methods. ISPRS Int J Geo-Inf 8:112.

SHCP, 2021. Proyecto de presupuesto de egresos de la Federación 2021. [Internet]. Available from: https://www.ppef.hacienda.gob.mx/work/models/PPEF2021/docs/12/r12_ppcer.pdf

Thurston H, Freisthler B, Bell J, Tancredi D, Romano PS, Miyamoto S,Joseph JG, 2017. The temporal-spatial distribution of seriously maltreated children. Spatial Spatio-temp Epidemiol 20:1-8.

Urquía-Fernández N, 2014. La seguridad alimentaria en México. Salud Públ México 56:s92-s98.

Vázquez JR, Ramírez JC, Rojas LA, Romero OC, Ledezma JCR, 2018. La obesidad y su asociación con otras de las enfermedades crónicas no transmisibles. J Negat No Positive Results JONNPR 3:627-42.

Villa-Mancera A, Pastelín-Rojas C, Olivares-Pérez J, Córdova-Izquierdo A, Reynoso-Palomar A, 2018. Bulk tank milk prevalence and production losses, spatial analysis, and predictive risk mapping of Ostertagiaostertagi infections in Mexican cattle herds. Parasitol Res 117:1613-20.

Villa-Mancera A and Reynoso-Palomar A, 2019. Bulk tank milk ELISA to detect IgG1 prevalence and clustering to determine spatial distribution and risk factors of Fasciola hepatica-infected herds in México. J Helminthol 93:704-10.

World Health Organization (WHO). Enfermedades no transmisibles. Nota Descriptiva. Diciembre 2021 [Internet]. WHO, Washington, DC, USA. Available from: https://www.who.int/es/news-room/fact-sheets/detail/the-top-10-causes-of-death

Zaragoza Bastida A, Hernández Téllez M, Bustamante Montes LP, Medina Torres I, Jaramillo Paniagua JN, Mendoza Martínez GD, Ramírez Durán N, 2012. Spatial and temporal distribution of tuberculosis in the State of México, México. Sci World J 2012:570278.